NOTICE CONCERNING COPYRIGHT RESTRICTIONS

Optimized EGS Reservoir Stimulation using Microseismic and Numerical Methods

Xueping Zhao[1], Juan M. Reyes-Montes[1], Jennifer R. Andrews[1], and R. Paul Young[2]

[1]Applied Seismology Consultants, Shrewsbury, U. K.
[2]University of Toronto, Toronto, Canada

Keywords

EGS reservoir, discrete element method, synthetic rock mass, synthetic seismicity, microseismic monitoring, natural fractures

ABSTRACT

In this paper, in order to develop robust predictive models for engineering the reservoir and the induced or mobilized fracture network, a fully dynamic 2D Synthetic Rock Mass model is validated to simulate fluid injection in a geothermal reservoir by comparing modeling geometries of hydraulic fractures and induced seismicity with actual results. The numerical results qualitatively agree with field observations and reveal the possible interaction between new fractures and natural fractures indicated by recorded microseimic events. The model enables us to examine in detail the interaction between fluid pressure, rock deformation and slip on existing fractures for the different reservoir conditions. The validated numerical models can help provide insight on the relationship between seismicity, stress/damage and the fluid front in order to optimize the EGS reservoir stimulation for the project in hand or for future projects.

1. Introduction

Passive microseismic (MS) monitoring provides a unique tool to monitor the evolution of fluid injection around the treated geothermal rock reservoir and seismic source mechanisms can yield information about the nature of deformation. However, there are still issues that cannot be understood from the MS data alone including: the relationship between the fluid migration; induced fractures; and MS locations. Furthermore, the conflict between induced tensile fractures suggested by theory (Economides and Nolte, 1989; Akulich and Zvyagin, 2008) and shear failure observed from recorded waveforms (Sasaki and Kaieda, 2002; Tischner et al., 2007) is still the subject of much interest. For these reasons, some attempts have been made to use the discrete element method (DEM) in which the rock is divided into deformable blocks or particles with fluid flowing between them (Jing et al., 2001). Hazzard and Young (2002) developed a DEM to model the fluid injection in a Hot Dry rock reservoir. They produced realistic fluid pressure histories and realistic seismic source parameters, but included a random network of joints rather than realistic joint geometries, and also did not consider the mechanical changes in domain volumes causing changes in domain pressures. In addition, their models were not able to simultaneously calibrate the unconfined compressive strength (UCS) and tensile strength of the rock, and the joint sliding between bonded particles in the previous models was not realistic due to the roughness or bumpiness induced by the particles.

The work presented here takes these models a step further by enabling fully fluid-mechanical coupling, using the latest developed synthetic rock mass model which has more flexibility in the choice of fracture networks, and allows calibration for both UCS and tensile strength. The objective of this paper is to optimize EGS reservoir stimulation by investigating the influence of different key parameters, such as in-situ stresses and fluid injection rates, on the distributions of induced fracture and MS events in an EGS reservoir at the Upper Rhine Graben similar to the Soultz site in France, the Landau site in German, the Basel site in Switzerland, and other geothermal reservoirs worldwide.

2. Method

2.1 Bonded Particle Model

Itasca's particle flow code (PFC) is a distinct element geomechanical modeling program using the bonded particle model (BPM) in which the rock material is modeled as an assembly of circular (2D) or spherical (3D) particles bonded together at their contacts by parallel-bonds (cement). Under the applied load, the bonds can break and a small crack can form. By further generation of these microcracks, a fracture can develop from the linking of individual microcracks. The micro-stiffness and micro-strength of particles can be adjusted to reproduce realistic macro-rock behavior. A thorough description of the PFC model for rocks was given by Potyondy and Cundall (2004). PFC has been applied to study mechanical behavior of sandstones, granites and other rocks under different stress conditions with much success, such as ther-

mal fracturing experiments (Wanne and Young, 2008), hydraulic fracturing (Al-Busaidi et al., 2005), seismic velocities (Hazzard and Young, 2004b), in-situ failure tests (Potyondy and Autio, 2001) and large-scale underground excavations (Cai et al., 2007).

However, the BPM suffered limitation because the UCS and tensile strengths of a typical hard rock cannot be matched simultaneously in a model. If the tensile strength was selected as the matching parameter, which is considered more important since hydrofracturing is predominantly a tensile process, the UCS of the model was much lower than that of the real rock. More recently, Potyondy (2010) has successfully overcome this limitation in 2D by simulating the actual grain shape of the rock making use of the smooth-joint contact model to represent the grain boundaries. The 2D grain-based models mimic deformable, polygonal grains cemented at their interfaces, and models with unbreakable grains match the macroscopic response of hard rock and most of the mechanisms that occur during direct tension and compression tests. This new update, referring to the enhanced model, will be applied to the model calibration in this paper.

2.2 Synthetic Rock Mass

In order to mimic pre-existing joints (natural fractures), a Synthetic Rock Mass (SRM) numerical model is developed. SRM samples model the movement and interaction between stressed assemblies of bonded non-uniform-sized disks in 2D or spheres in 3D (BPM created from PFC) with an embedded discrete network of disc-shaped flaws (Discrete Fracture Network) that reproduce the pre-existing joint fabric (representing joints, faults or other pre-existing fractures as smooth, frictional (or cohesive) planar features) (Pierce et al., 2007; Pierce, 2010). Each individual joint is represented explicitly within the SRM sample making use of the recently developed smooth-joint contact model (SJM) (Mas Ivars et al., 2008 and 2011). The smooth-joint model simulates the behavior of an interface regardless of the local particle contact orientations along the interface. The behavior of a frictional or bonded joint can be modeled by assigning smooth-joint models to all contacts between particles that lie on opposite sides of the joint (Itasca, 2008). SRM samples that are subjected to the same mechanical or fluid disturbance expected in the field produce synthetic seismicity that can be compared directly with microseismic data collected in the field.

2.3 Synthetic Seismicity in PFC

PFC uses an explicit approach to solve the equation of motion. This allows a dynamic simulation in which seismic waves propagate out from new faults and fractures. Each bond breakage is assumed to be a microcrack. The crack location is assumed to be the contact between the two particles, and the orientation of the crack is assumed to be perpendicular to the line joining the two centers. When a bond breaks, part of the stored strain energy is released in the form of a seismic wave. Microcracks occurring closely in both space and time are considered a single seismic event, if the models are run dynamically, by specifying low levels of numerical damping that simulates realistic levels of attenuation in the rock (Hazzard and Young, 2004a). Seismic source information can therefore be calculated for seismicity. A numerical modeling technique to link the mechanics of fracture formation and the resulting seismicity was described by Hazzard and Young (2002). This technique calculates the moment tensor (source mechanism) for each event by summing the different components of moment at the contacts surrounding the source. The moment magnitude is then computed from elements of the moment tensor matrix (Feignier and Young, 1992). An example of a synthetic seismic event is illustrated in Figure 1. This work has been developed in order to integrate and correlate microseismic field observations with simulated microseismicity from numerical models using the discrete element method.

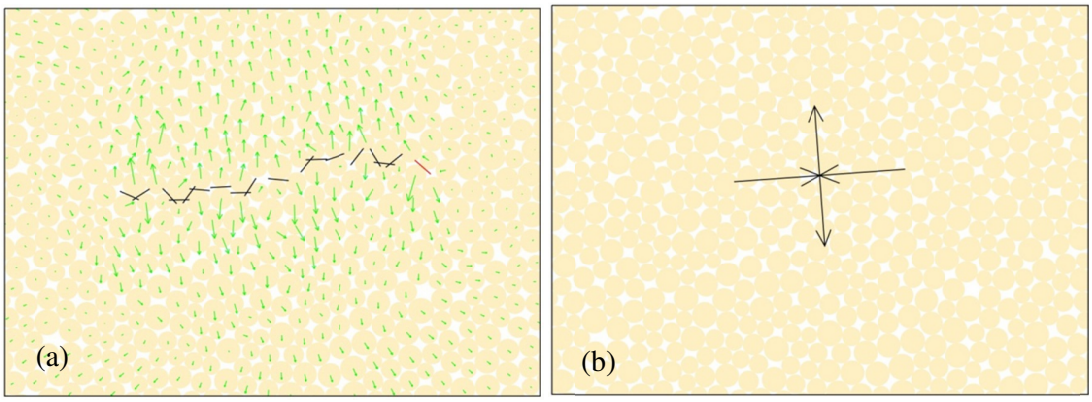

Figure 1. An example synthetic seismic shear event composed of 17 tensile cracks and 1 shear crack. (a) Particle velocities (green arrows) and cracks (black line for tensile crack and red line for shear crack); (b) the calculated moment tensor.

2.4 Fluid Flow Modeling in PFC

A technique for simulating fluid flow in PFC is adapted from the algorithm by Cundall (2000). Cundall's fluid flow is simulated by assuming that each particle contact is a flow channel (pipe) and that these channels connect up small "reservoirs" that store some fluid pressure. As shown in Figure 2, the fluid network topology is generated by drawing lines between the centers of all particles in contact. This creates a series of enclosed domains. The center of each of these domains is stored as a "reservoir". The reservoirs are then connected by flow pipes. One pipe exists for each particle contact. Therefore, each reservoir is surrounded completely by contacts and has some volume associated with it. For a 2D fluid network model, fluid flow through a

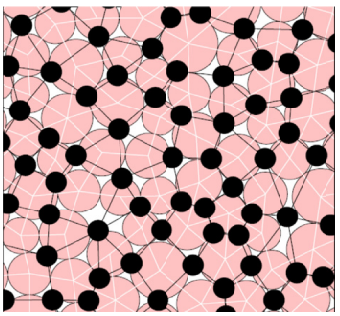

Figure 2. Reservoirs (black dots), flow pipes (black lines) and contacts (white lines) in compacted bonded assembly of particles in PFC2D.

pipe is approximated by laminar flow through parallel plates with some aperture associated with it. The rate of volumetric flow is controlled by the Darcy's law (Bear, 1972). A thorough description of the mathematical equations for the fluid network in PFC was given by Al-Busaidi et al. (2005) and Zhao (2010).

Hazzard and Young (2002) and Al-Busaidi et al. (2005) considered the mechanical change in domain volume negligible and did not include it in the calculation of domain pressure changes. However, in this paper we consider full hydro-mechanical coupling because, in reality, the pressure variation caused by domain volumetric change could be significant especially for the areas with induced and natural fractures.

3. Numerical Modeling Fluid Stimulations in an EGS Reservoir

3.1 Data Collection and Model Calibration

A Hot Dry Rock research program has been in place at Soultz-sous-Forêts (France) since 1987 (Baria et al., 1999). The project was renamed Enhanced Geothermal System (EGS) after it was established that the fractured granite contained large volume of hot saline fluid (Dorbath et al., 2009). At this site, water has been circulated through deep, hot, fractured granites with the aim of studying the feasibility of efficiently extracting geothermal energy. A wealth of microseismic data has been collected during these circulation tests and sophisticated location techniques have been applied (Phillips, 2000; Moriya et al., 2003; Cuenot et al., 2008; Dyer et al., 2008). Data acquisition and microseismic processing are used to map a disturbed or enlarging fracture network in space, magnitude and evolution (Andrews et al., 2011). The feedback provides "first order" information to engineers, potentially in real time, so that decisions on project design can be made and revised effectively and efficiently. Because of this wealth of data, it is proposed that simulating the Soultz experiment would be an excellent way to test the new modeling technique described here.

Before modeling the fluid injection, the BPM has to be initially calibrated by a set of biaxial and Brazilian tensile tests to fit the macro-properties of the laboratory rock (Soultz granite), such as UCS, tensile strength, Young's modulus, and Poisson's ratio. The best-fit parameters and calibration results are shown in Table 1, which indicates that the macro-properties are well reproduced by the enhanced BPM model.

Table 1. BPM calibration results.

Parameters	Actual*	Model
Young's modulus (GPa)	64	66.3
Poisson's ratio	0.285	0.274
UCS (MPa)	100-130	118.9
Tensile strength (MPa)	19.4	18.5

* From Valley and Evans (2007)

The calibrated BPM was then created to simulate a 2D slice of the Soultz reservoir approximately 2 km below the surface. The 1 km × 1 km reservoir model was made up of 18,389 particles with an average radius of 3.8 m to optimize calculation time (Figure 3). Clearly each particle does not represent a single mineral grain in the rock and the particles are simply a way to discretize the medium. A physical interpretation of the particles might be a block of granite separated by cohesive planes of weakness.

According to the natural fracture network in the Soultz granite described by Dezayes et al. (2005), natural fractures are nearly vertical with dominant orientation close to north-south and dominant dipping to the east, and all natural fractures are filled or partly filled by hydrothermal secondary minerals, such as clays, calcite, and quartz, etc. In addition, the in-situ maximum horizontal stress is about N140-170E (Dyer et al., 2008). In order to qualitatively simulate the main features of natural fractures, a SRM model was created by including three sets of representative pre-existing natural fractures. As shown in Figure 3, these fractures were modeled as smooth joints in order to mimic the two main fracture groups strike N20E and N30W (Phillips, 2000). Table 2 lists the parameters defining the dimensions of these joints. Furthermore, to account for the filled minerals, particles within joints were bonded together with less tensile strength and cohesion compared to their intact values, at the same time, among the natural fractures the permeability was considered to be less than that outside of the fractures.

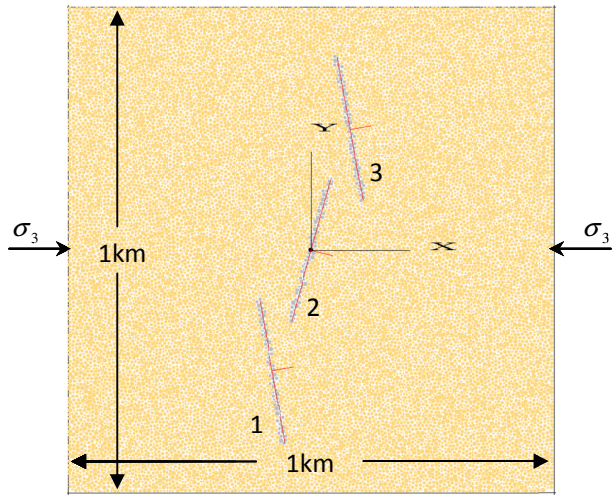

Figure 3. 2D SRM model with three sets of numbered pre-existing natural fractures. The center of the sample at x=0 and y=0 is selected as fluid injection point. The particles within the pre-fracture are colored in grey. The smooth joints are marked by a longer red line (at the joint center oriented parallel with the joint surface) and a red shorter line (indicating the orientation of the joint plane).

Table 2. Parameters for pre-existing natural fractures in SRM models.

Parameters	Units	Natural Fracture 1	Natural Fracture 2	Natural Fracture 3
Dip*	degree	80	105	80
Center (x, y)	m	(-80,-250)	(0,0)	(80,250)
Length	m	150	150	150

* The dip angle is measured from the positive x-direction to the joint surface in a clockwise direction.

As shown in Figure 3, σ_1 and σ_3 are maximum and minimum horizontal stresses, respectively. Stresses are applied at the boundaries of the model by walls acting under a servo-mechanism. Note that effective stress is assumed so that the applied stresses, σ_1 and σ_3, equal the actual in-situ stresses minus the pore fluid pressure.

3.2 Model Results and Discussion

Field stimulation can generate thousands of MS events and, critically, a few small earthquakes that may be felt at the surface. In addition, the earthquake magnitudes may determine if development of the reservoir is even possible (i.e., if the magnitudes exceed local limits or cause public concern) (Dyer et al., 2008). Therefore, in order to evaluate the potential for developing a fractured reservoir, the injection parameters have to be optimized. Generally, the in-situ stress and fluid injection rate have the strong influence on the distributions of the induced fracture network and MS events. Here, three different injection rates (q_i) and in-situ stresses were tested as listed in Table 3.

The rate of injection in the model was calculated by assuming that the fluid flows approximately 2 km in the vertical direction. A typical rate of flow that induces fracturing in the Soultz site is 40 l/s (Valley and Evans, 2007). If this is converted to m^3/s and divided by 2000, then an injection rate of 2×10^{-5} m^3/s results. Note that the injection rate used in the model is much larger than the actual value at the Soultz site, because the current coarse model has a larger particle size than the actual grain size (Hébert et al., 2011). According to the studies by Potyondy and Cundall (2004), the fracture toughness scaling goes by the product of the tensile strength and the square root of the grain size for real rocks. Therefore, the fracture toughness of the current model is about two orders of magnitude larger than that of the real rocks. As a result, the injection rate in the PFC model cannot be easily related to the actual injection rate because of higher fracture toughness and the 2D nature of the model, so a rate was chosen that was fast enough to induce fracturing and result in reasonable model run times, but slow enough to maintain stability. As shown in Table 3, the injection rate of 2×10^{-3} m^3/s was tested as the base for all three in-situ stress combinations, and other two injection rates were only tested for the reservoir model with $\sigma_1 = \sigma_3 = 3$ MPa.

Table 3. Fluid injection parameters in SRM models.

Parameters	Units	Actual*	Model
σ_1 / σ_3	MPa	20/3	20/3, 9/3, 3/3
q_i	m^3/s	2×10^{-5}	2×10^{-3}, 4×10^{-3}, 8×10^{-3}

* From Valley and Evans (2007)

Figures 4 to 8 show all model results with different in-situ stresses and fluid injection rates. As shown in Figure 4, it is interesting that the MS events first propagated along the center joint, and then detoured parallel to the upper and lower joints, until the new cluster of MS events were induced parallel to the σ_1 direction when new fractures passed the upper and lower joints. Due to the high in-situ differential stress and low angle of approach, the induced MS events and fractures were arrested by the pre-existing fracture. This interaction mode between the induced fractures and pre-existing fracture is consistent with Blanton's (1986), Warpinski and Teufel's (1987) and Zhou's (2008) experimental results, and also Zhao's (2010) numerical results. As shown in Figure 4(b), the induced fractures were usually opened perpendicular to the joint surface within the range of joints, and parallel to the σ_3 direction beyond the pre-existing joints as expected. Furthermore, the higher fluid pressure (permeable zone) was accumulated between the upper and lower joints, and the structures for induced fractures are more complicated in front of the pre-existing joints but constrained by the permeable zone. Note that the induced cracks at the edge of the model are more scattered, which may be due to the edge effect and need more study, probably a larger reservoir model.

Compared to Figure 4, Figure 5 clearly shows the effect of the in-situ stress on the induced MS and fractures. Within a similar injection time, the higher the differential stress, the farther fracture half-length will be induced, the higher magnitude for MS events will be triggered, the less pervasive fluid network will be produced, and the higher the likelihood that the fracture tip will go ahead of the fluid front. Moreover, as shown in Figures 5(c) and (d), after the fluid was injected for longer, MS events also showed a trend propagating parallel to the upper and lower pre-existing joints when induced fractures interacted with them. The difference between Figure 4(a) and Figure 4(c) is that more MS events were

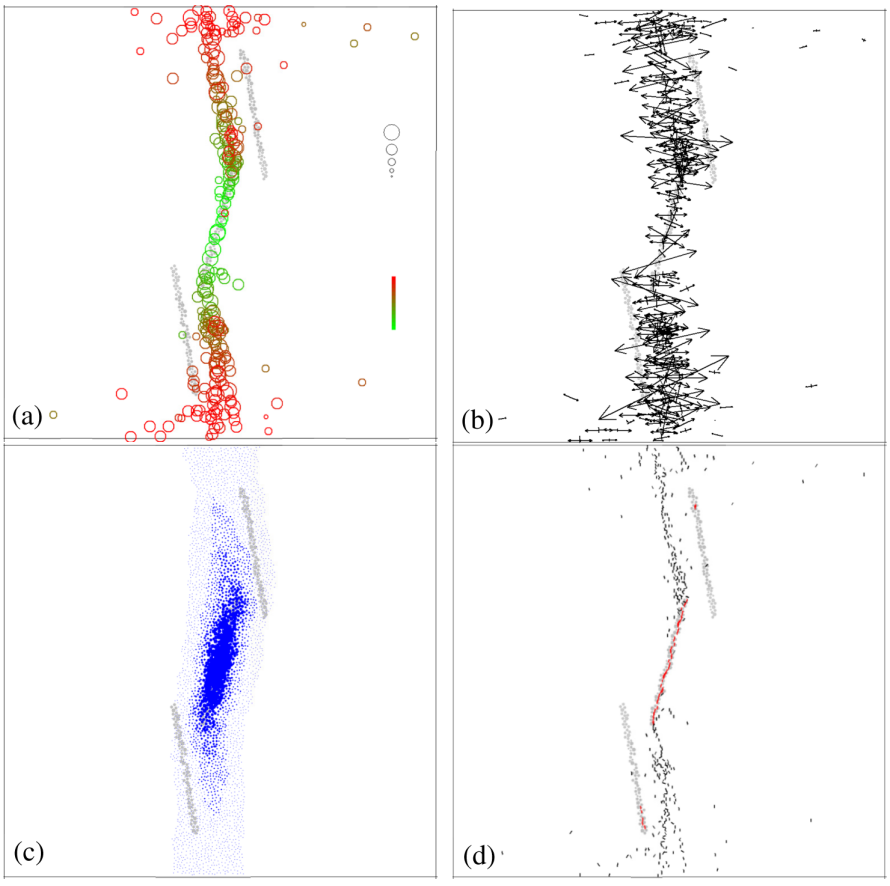

Figure 4. Synthetic MS, moment tensors, fluid flow and induced cracks for the SRM model with σ_1=20 MPa, σ_3 =3 MPa and q_i=2×10^{-3} m^3/s after fluid injection about 34.4 hours. The dimension of each subfigure is 1 km × 1 km (a) Synthetic MS events. The sizes of seismic events are scaled to magnitudes between -1.3 to 0.52 and the color corresponds to the occurring time of seismic events (green/red=early/late). (b) Moment tensors corresponding to (a). (c) Fluid pressure (blue circles whose sizes are scaled to 50 MPa). (d) Induced cracks (black/red lines correspond to cracks induced outside/inside of smooth joints).

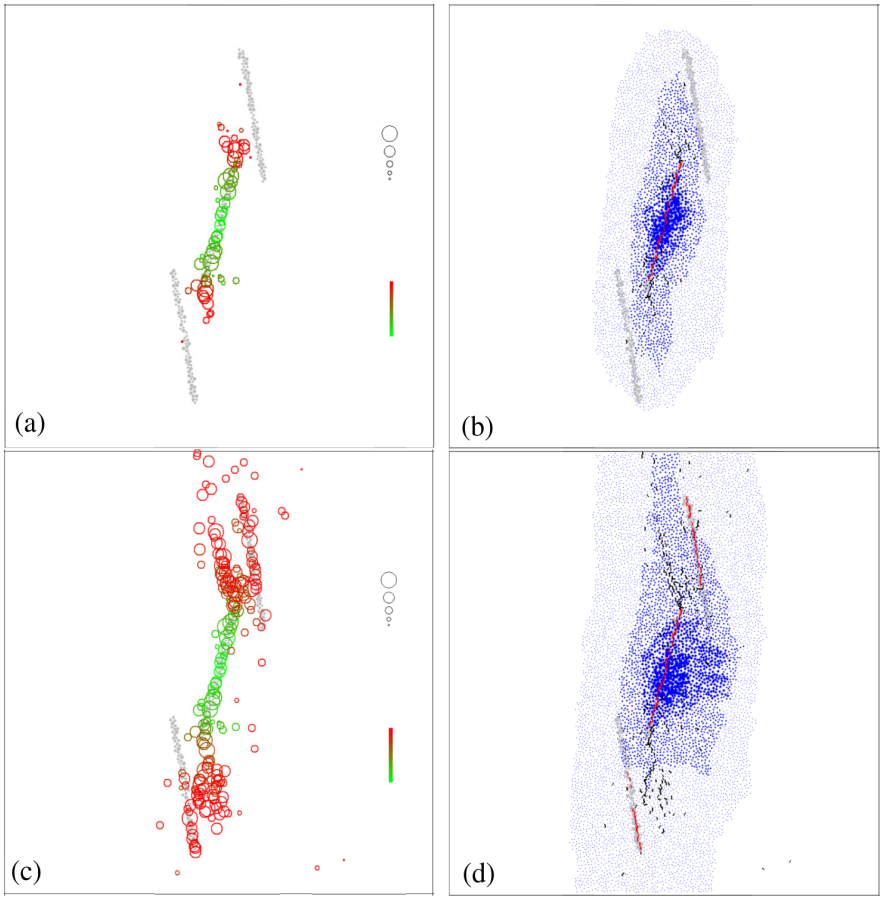

Figure 5. Synthetic MS, fluid flow and induced cracks for the SRM model with σ_1 =9 MPa, σ_3=3 MPa and q_i=2×10^{-3} m^3/s after fluid injection about 35.1 hours for (a) and (b) and 63.8 hours for (c) and (d). The dimension of each subfigure is 1 km ×1 km. (a) Synthetic MS events. The sizes of seismic events are scaled to magnitudes between -0.63 to 0.36 and the color corresponds to the occurring time of seismic events (green/red=early/late). (b) Fluid pressure (blue circles whose sizes are scaled to 50 MPa) and induced cracks (black/red lines correspond to cracks induced outside/inside of smooth joints). (c) Synthetic MS events. The sizes of seismic events are scaled to magnitudes between -0.94 to 0.46 and the color has the same meaning as that in (a). (d) Fluid pressure and induced cracks whose marks have the same meanings as those in (b).

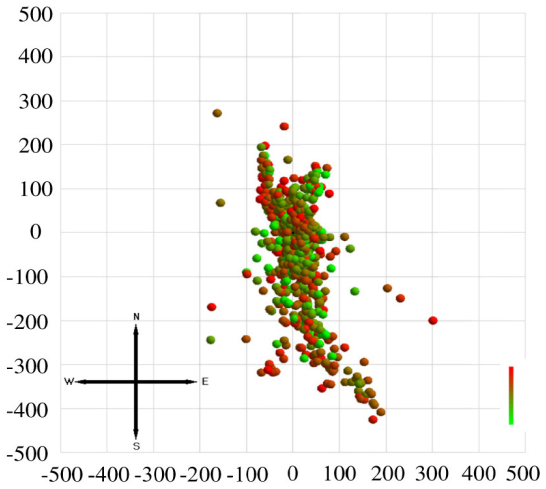

Figure 6. Plan view of 901 events from the September 8-10, 1993 experiment at Soultz. The color corresponds to the occurring time of MS events (green/red=early/late). Each grid is 100 m×100m.

triggered within the pre-existing joints, indicating that more slip could be caused at the lower in-situ differential stress compared to the number of induced cracks within the pre-existing joint as shown in Figure 4(d) and Figure 5(d).

Figure 6 shows the plan view of MS events recorded during the fluid injection within September 8-10, 1993 in the well GPK1 at Soultz (Andrews et al., 2011). Compared to the field record in Figure 6 and synthetic MS events in Figures 4(a) and 5(c), both show the similar propagating patterns with regard to MS events, such as event locations with time, linear orientations, and truncation or arrestment of events in the N-E and S-W directions. The same truncating phenomenon of MS events was also found by Phillips (2000). This reasonable comparison reveals that natural fractures could be the physical reason causing the arrestment of the propagation of seismic events, and that the linear clusters of MS are usually related to pre-existing fractures in a geothermal reservoir, but they may have some offsets in the distance depending on the geometry of natural fractures and in-situ stresses. Understanding these mechanisms could help interpret recorded MS and make commercial EGS operations more cost effective.

Besides the high in-situ stress ratio, the hydrostatic reservoir model was also tested. As shown in Figure 7, although no fracture was produced under the hydrostatic stress with the base injection rate, the non-linear fluid network indicates the potential for the non-linear propagation of MS events. In order to verify this hypothesis, two higher injection rates were tested under the same hydrostatic stress state. As shown in Figures 8 and 9, by increasing the injection rate, the number of MS events and their magnitudes increase and their special distributions become more complex. At the same time, the fluid network becomes more irregular without the constraint by the pre-existing joints. Therefore, the higher

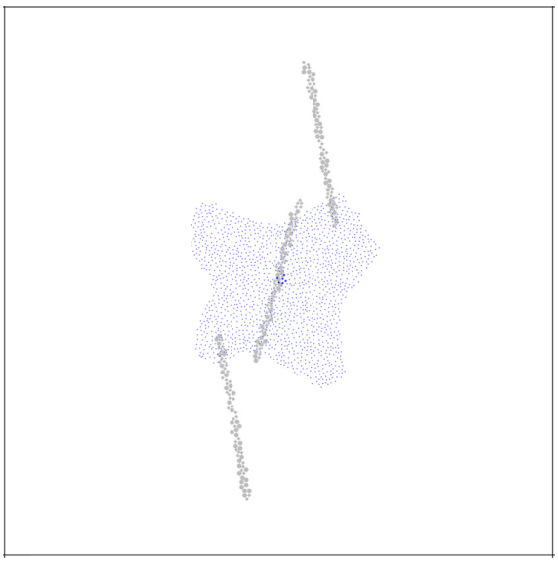

Figure 7. Fluid pressure (blue circles whose sizes are scaled to 50MPa) for the SRM model with σ_1 =3 MPa, σ_3 =3 MPa and q_i=2×10^{-3} m^3/s after fluid injection about 8.1 hours.

injection rate will be needed in order to produce a more pervasive fracture network. Furthermore, the less differential stress, the more multiple branches for induced fractures as indicated from Figures 4, 5 and 9.

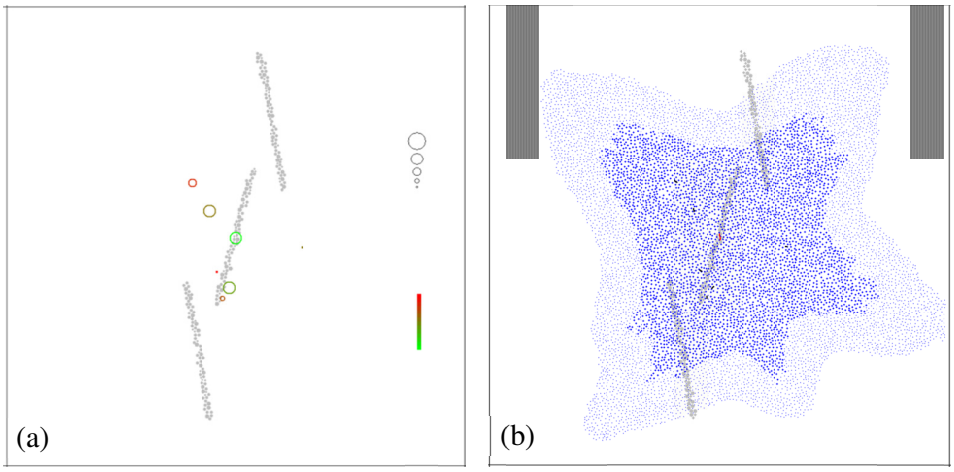

Figure 8. Synthetic MS, Fluid flow and induced cracks for the SRM model with σ_i=3 MPa, σ_3 =3 MPa and q_i=4×10^{-3} m^3/s after fluid injection about 34.6 hours. The dimension of each subfigure is 1 km×1 km. (a) Synthetic MS events. The sizes of seismic events are scaled to magnitudes between -0.93 to -0.11 and the color corresponds to the occurring time of seismic events (green/red=early/late). (b) Fluid pressure (blue circles whose sizes are scaled to 50 MPa) and induced cracks (black/red lines correspond to crack s induced outside/inside of smooth joints).

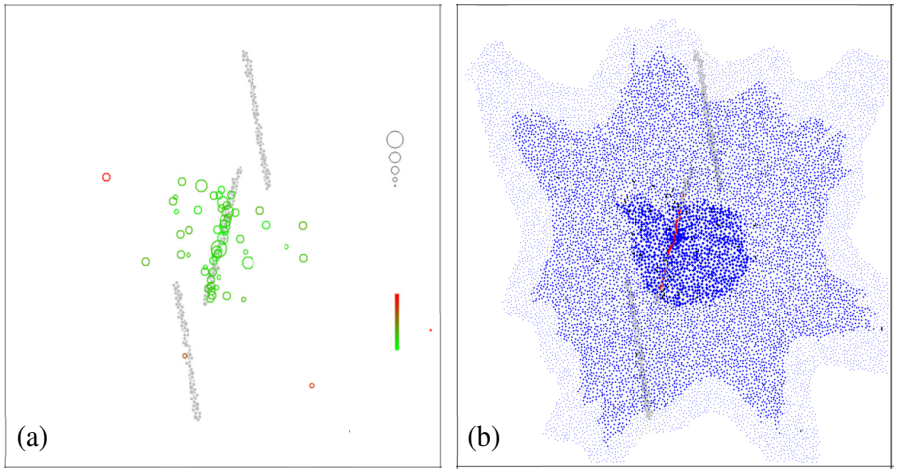

Figure 9. Synthetic MS, Fluid flow and induced cracks for the SRM model with σ_i=3 MPa, σ_3 =3 MPa and q_i=8×10^{-3} m^3/s after fluid injection about 32.4 hours. The dimension of each subfigure is 1 km×1 km. (a) Synthetic MS events. The sizes of seismic events are scaled to magnitudes between -0.98 to 0.39 and the color corresponds to the occurring time of seismic events (green/red=early/late). (b) Fluid pressure (blue circles whose sizes are scaled to 50 MPa) and induced cracks (black/red lines correspond to cracks induced outside/inside of smooth joints).

Conclusions

In this paper, a fully dynamic 2D Synthetic Rock Mass (SRM) model was successfully validated to simulate fluid injection in a geothermal reservoir with strong crystalline rocks present in the Rhine Graben region by directly comparing modeling geometries of hydraulic fractures and induced seismicity with actual results. The numerical results qualitatively agree with field observations and reveal the possible interaction between new fractures and natural fractures indicated by recorded microseimic events.

Two key parameters, in-situ stress and fluid injection rate, were examined in order to test the EGS reservoir response and optimize the fluid injection. The numerical results revealed that the higher differential stress, the farther induced fracture half-length, the less multiple branches for induced fractures, the higher magnitude for MS events, the less pervasive fluid network, and the higher the likelihood that the fracture tip will go ahead of the fluid front. Furthermore, the higher injection rate, the more MS events with a higher magnitude, and the more pervasive fluid network and induced fractures.

The model has demonstrated the ability to better interpret the causal effects of the microseismicity by analysing the micromechanics occurring within the numerical model framework (recognising that in the model we observe all activity within the configured boundary conditions, whereas field observations record only a portion of the activity depending on the sensitivity of the monitoring system). The validated numerical models can help elucidate our understanding of the mechanics underlying seismicity, and examine in detail the interaction between fluid pressure, rock deformation and slip on existing fractures.

Admittedly, the model is still a gross simplification of the actual situation. In particular, the low resolution, the 2D nature of the models, and the shortage of actual natural fracture network limit the possible quantitative comparisons with actual data. However, through the use of synthetic seismicity, moment tensors, and fractures, the current model clearly demonstrates not only the reasonable physical mechanics underlying the interaction between hydraulic and natural fractures, but also the relationship between the fluid front and the fracture tip, all of which are difficult to ascertain from field data. If a high resolution was used, the model would produce a realistic injection rate and more synthetic seismicity for better comparisons with field data. Moreover, modeling results in 2D may not be fully representative of fluid properties (fluid volume and injection fluid rate) and, thus, of the total number of induced microcracks. 3D modeling is more realistic, allowing the use of a realistic fluid injection rate and examination of both lateral and vertical hydrofracture growth, especially for reservoirs with natural fractures, such as EGS reservoirs.

References

Akulich, A. V., and A. V. Zvyagin, 2008. "Interaction Between Hydraulic and Natural Fractures." *Fluid dynamics*, v.43, p.428-435.

Al-Busaidi, A., J. F. Hazzard, and R. P. Young, 2005. "Distinct Element Modeling of Hydraulically Fractured Lac du Bonnet Granite." *J. Geophys. Res.*, v.110, B06302.

Andrews, J. R., J. M. Reyes-Montes, and R. P. Young, 2011. "Continuous Microseismic Record Analysis for Reservoir Hydrofracture Treatments." Geothermal Resources Council *Transactions*.

Baria. R., J. Baumgärtner, A. Gérard, R. Jung, and J. Garnish, 1999. "European HDR Research Programme at Soultz-sous-Forêts (France) 1987-1996." *Geothermics,* v.28, p.655-669.

Bear, J., 1972. "Dynamics of Fluids in Porous Media." American Elsevier Publishing Company, Inc.

Cai, M., P. K. Kaiser, H. Morioka, M. Minami, T. Maejima, Y. Tasaka, and H. Kurose, 2007. "FLAC/PFC Coupled Numerical Simulation of AE in Large-scale Underground Excavations." *Int. J. Rock Mech. & Min. Sci.*, v.44, p.550-564.

Cuenot, N., C. Dorbath, and L. Dorbath, 2008. "Analysis of the Microseismicity Induced by Fluid Injections at the Hot Dry Rock Site of Soultz-sous-Forêts (Alsace, France): Implications for the Characterization of the Geothermal Reservoir Properties." *Pure Appl. Geophys.*, v.165, p.1-32.

Cundall, P., 2000. "Fluid Formulation for PFC2D." Itasca Consulting Group.

Dezayes, C., B.Valley, E. Maqua, G. Syren, and A. Genter, 2005. "Natural Fracture System of the Soultz Granite Based on UBI Data in the GPK3 and GPK4 Wells." *Proceedings* of the EHDRA Scientific Conference.

Dorbath, L., N. Cuenot, A. Genter, and M. Frogneux, 2009. "Seismic Response of the Fractured and Faulted Granite of Soultz-sous-Forêts (France) to 5 km Deep Massive Water Injections." *Geophys. J. Int.*, v.177, p.653-675.

Dyer, B. C., U. Schanz, F. Ladner, M. O. Haring, and T. Spillman, 2008. "Microseismic Imaging of a Geothermal Reservoir Stimulation." *The Leading Edge*, v.27, p.856-869.

Economides, M. J., and K. G. Nolte, 1989. "Reservoir Stimulation (second edition)." Prentice Hall.

Feignier, B., and R. P. Young, 1992. "Moment Tensor Inversion of Induced Microseismic Events–Evidence of Nonshear Failures in the -4<M<-2 Moment Magnitude Range." *Geophys. Res. Lett.*, v.19, p.1503-1506.

Hazzard, J. F., and R. P. Young, 2004a. "Dynamic Modelling of Induced Seismicity." *Int. J. Rock Mech. & Min. Sci.*, v.41, p.1365-1376.

Hazzard, J. F., and R. P. Young, 2004b. "Numerical Investigation of Induced Cracking and Seismic Velocity Changes in Brittle Rock." *Geophys. Res. Lett.*, v.31, L01604.

Hazzard, J. F., R. P. Young, and S. J. Oates, 2002. "Numerical Modelling of Seismicity Induced by Fluid Injection in a Fractured Reservoir." *Proceedings* of 5th North American Rock Mechanics Symposium, NARMS-TAC, p.1023-1030.

Hébert, R. L., B. Ledésert, A. Genter, D. Bartier, and C. Dezayes, 2011. "Mineral Precipitation in Geothermal Reservoir: the Study Case of Calcite in the Soultz-sous-Forêts Enhanced Geothermal System." *Proceedings* of Thirty-Sixth Workshop on Geothermal Reservoir Engineering, Stanford University, California, SGP-TR-191.

Itasca Consulting Group Inc., 2008. "PFC2D-Particle Flow Code in 2D Dimensions, Version 4.0." Minneapolis.

Jing, L., Y. Ma, and Z. Fang, 2001. "Modeling of Fluid Flow and Solid Deformation for Fractured Rocks with Discontinuous Deformation Analysis (DDA) Method." *International Journal of Rock Mechanics and Mining Sciences*, v.38, p.343–355.

Mas Ivars, D., M. Pierce, C. Darcel, J. Reyes-Montes, D. O. Potyondy, R. P. Young, and P. A. Cundall, 2011. "The Synthetic Rock Mass Approach for Jointed Rock Mass Modeling." *Int. J. Rock Mech. & Min. Sci.*, v.48, p.219-244.

Mas Ivars, D. D. O. Potyondy, M. Pierce, and P. A. Cundall, 2008. "The Smooth-Joint Contact Model." *Proceedings* of the 8th world congress on computational mechanics/5th European congress on computational methanics and applied science and engineering, Venice, paper a2735.

Moriya, H., H. Niitsuma, and R. Baria, 2003. "Estimation of Fine Scale Structures in Soultz HDR Reservoir by Using Microseismic Multiplets." *Proceedings* of Twenty-Eighth Workshop on Geothermal Reservoir Engineering, Stanford University, SGP-TR-173.

Phillips, W. S., 2000. "Precise Microearthquake Locations and Fluid Flow in the Geothermal Reservoir at Soultz-sous-Forêts, France." *B. Seismol. Soc. Am.*, v.90, p. 212-228.

Pierce, M., 2010. "Keynote on fracture network engineering." *Proceedings* of 44th US Rock Mechanics Symposium, American Rock Mechanics Association.

Pierce, M., P. Cundall, D. Potyondy, and D. Mas Ivars, 2007. "A Synthetic Rock Mass Model for Jointed Rock, in E. Eberhardt et al., eds., Rock Mechanics: Meeting Society's Challenges and Demands (1st Canada-U.S. Rock Mechanics Symposium) Vol. 1: Fundamentals, New Technologies & New Ideas." Taylor & Francis Group.

Potyondy, D., 2010. "BPM Improvements to Match Macroproperties of Hard Rock." Itasca Consulting Group, Inc., Minneapolis, MN, Technical Memorandum ICG6862-L.

Potyondy, D., and J. Autio, 2001. "Bonded-Particle Simulations of the In-Situ Failure Test at Olkiluoto." *Proceedings* of 38th U.S. Rock Mechanics Symposium.

Potyondy, D., and P. A. Cundall, 2004. "A Bonded-Particle Model for Rock." *Int. J. Rock Mech. & Min. Sci.*, v.41, p.1329-1364.

Sasaki, S., and H. Kaieda, 2002. "Determination of Stress State from Focal Mechanisms of Microseismic Events Induced During Hydraulic Injection at the Hijiori Hot Dry Rock Site." *Pure Appl. Geophys.*, v.159, p.489-516.

Tischner, T., M. Schindler, R. Jung, and P. Nami, 2007. "HDR Project Soultz: Hydraulic and Seismic Observations During Simulation of the 3 Deep Wells by Massive Water Injections." *Proceedings* of 32nd Workshop on Geothermal Reservoir Engineering.

Valley, B. and K. F. Evan, 2007. "Stress State at Soultz-sous-Forêts to 5 km Depth from Wellbore Failure and Hydraulic Observations." *Proceedings* of Thirty-Second Workshop on Geothermal Reservoir Engineering, Stanford University, California, SGP-TR-183.

Wanne, T. S., and R. P. Young, 2008. "Bonded-Particle Modeling of Thermally Fractured Granite." *Int. J. Rock Mech. & Min. Sci.*, v.45, p.789-799.

Zhao, X. P., 2010. "Imaging the Mechanics of Hydraulic Fracturing in Naturally-Fractured Reservoirs Using Induced Seismicity and Numerical Modeling." *Ph.D. thesis*, University of Toronto.